

**This is an ACCEPTED VERSION of the following published document:**

R. Maneiro-Catoira, J. Brégains, J. A. García-Naya and L. Castedo, "Dual-Signal Transmission Using RF Precoding and Analog Beamforming With TMAs," in *IEEE Communications Letters*, vol. 22, no. 8, pp. 1640-1643, Aug. 2018, doi: 10.1109/LCOMM.2018.2848274.

Link to published version: <https://doi.org/10.1109/LCOMM.2018.2848274>.

**General rights:**

© 2018 IEEE. This version of the article has been accepted for publication, after peer review. Personal use of this material is permitted. Permission from IEEE must be obtained for all other uses, in any current or future media, including reprinting/republishing this material for advertising or promotional purposes, creating new collective works, for resale or redistribution to servers or lists, or reuse of any copyrighted component of this work in other works. The Version of Record is available online at: <https://doi.org/10.1109/LCOMM.2018.2848274>.

# Dual-Signal Transmission using RF Precoding and Analog Beamforming with TMAs

Roberto Maneiro-Catoira, *Member, IEEE*, Julio Brégains, *Senior Member, IEEE*,  
José A. García-Naya\*, *Member, IEEE*, and Luis Castedo, *Senior Member, IEEE*

**Abstract**—Time-Modulated Arrays (TMAs) receive beamforming provides a noteworthy hardware simplicity given the ability of this multi-antenna technique to transform spatial diversity into frequency diversity. However, the dual behavior at transmission seems to be as simple as limited: a given signal is simultaneously transmitted over all the different TMA harmonic patterns. We investigate the efficient and simultaneous transmission of two different signals over the same physical antenna using two independent harmonic beam-patterns of the TMA. For that purpose, we propose an innovative dual-signal TMA transmitter based on two complementary operations: the complex mixing of the baseband signals and the TMA processing with quadrature and time-delayed periodic pulses.

**Index Terms**—Antenna arrays, time-modulated arrays, beamforming, spatial diversity.

## I. INTRODUCTION

TIME-Modulated Arrays (TMAs) are easily reconfigurable radiating systems originally implemented with fast radio frequency (RF) switches [1]. Most research on TMAs focuses on its use at reception (e.g., [1], [2]), while less attention has been paid to its transmit mode operation. The frequency restrictions to keep the transmit signal integrity, as well as its radiated power, were determined in [3]. The transmission of narrowband analog and digital signals over the fundamental mode pattern of the TMA was analyzed in [4] and [5], respectively. The transmission of direction-dependent signals using the harmonic patterns was addressed in [6], whereas the multibeam characteristics of TMAs for space-division multiple access (SDMA) were studied in [7]. However, none of the above-mentioned works addressed the fundamental problem of avoiding the transmit/receive power losses over unwanted (but inherently generated) TMA harmonic patterns when applied to wireless communications.

Therefore, the efficient use of the TMA harmonic beamforming features for dual-signal transmission purposes is still an unexplored field. The main contribution of this letter is, precisely, to address the modeling of a dual-input TMA that allows for simultaneously transmitting two baseband complex signals over the same frequency and the same physical antenna

\* Corresponding author: José A. García-Naya.

This work has been funded by the Xunta de Galicia (ED431C 2016-045, ED341D R2016/012, ED431G/01), the Agencia Estatal de Investigación of Spain (TEC2015-69648-REDC, TEC2016-75067-C4-1-R) and ERDF funds of the EU (AEI/FEDER, UE).

The authors are with the University of A Coruña, Spain. E-mail: roberto.maneiro@udc.es, julio.bregains@udc.es, jagarcia@udc.es, luis@udc.es

Digital Object Identifier

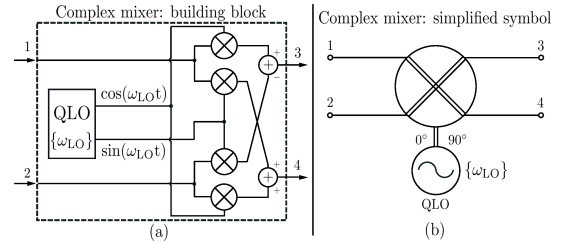


Fig. 1. (a) Building block of a complex mixer, and (b) its corresponding simplified symbol. LO stands for local oscillator, QLO stands for quadrature local oscillator, and  $\omega_{LO}$  is the frequency of the local oscillator.

array, but with the benefit of offering independent reconfigurability of their spatial signatures.

Such a basic layout is based on two techniques that perform a complex mixing followed by a TMA processing. The complex mixing is carried out using two building blocks (see Fig. 1) forming the dual complex mixer shown in Fig. 2. The complex mixer pre-processes the baseband signals to produce two output signals: (a) an in-phase signal consisting of the original ones located at two different carrier frequencies  $\omega_{c1}$  and  $\omega_{c2}$ , and (b) a quadrature signal composed of a  $+\pi/2$  phase shifted version of the first one and a  $-\pi/2$  phase shifted version of the second one, both located at carrier frequencies  $\omega_{c1}$  and  $\omega_{c2}$ , respectively. In this technique, complex mixing can be interpreted as an analog precoding of the signals to be transmitted in order to efficiently exploit the subsequent transformations carried out by the TMA. A dual-input TMA is required to process the above-mentioned quadrature signals (see Fig. 3). Through time modulation (TM), we pursue a two-fold objective: (1) to design a single side band (SSB) TMA which only radiates over the positive working harmonics, thus duplicating its efficiency; and (2) to transmit each signal over a different harmonic pattern in such a way that we endow each transmitted signal with a different spatial signature. The first objective is attained by applying an in-parallel TM to each antenna input with a given pulse and its Hilbert transform (HT) followed by a  $\pi/2$  phase shifting (see Fig. 3). The second objective requires the pulses at the quadrature input be time-delayed with respect to the in-phase ones. The applied periodic pulses are pre-processed rectangular pulses due to their versatility and ability to safeguard the antenna efficiency.

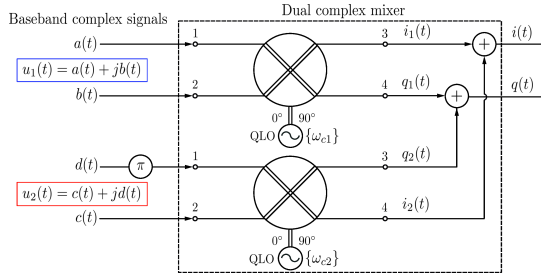


Fig. 2. Block diagram of the dual complex mixer (with carrier frequencies  $\omega_{c1}$  and  $\omega_{c2}$ ) that pre-processes two generalized complex baseband signals to be transmitted over the dual-input SSB TMA.

## II. A SIMPLE ANALOG PRECODING: COMPLEX MIXING

By virtue of the schemes shown in Fig. 1, the signals at the output of each complex mixer (see Fig. 2) are given by

$$\begin{aligned} i_1(t) &= a(t)\cos(\omega_{c1}t) - b(t)\sin(\omega_{c1}t), \\ q_1(t) &= a(t)\sin(\omega_{c1}t) + b(t)\cos(\omega_{c1}t), \\ i_2(t) &= c(t)\cos(\omega_{c2}t) - d(t)\sin(\omega_{c2}t), \text{ and} \\ q_2(t) &= -d(t)\cos(\omega_{c2}t) - c(t)\sin(\omega_{c2}t), \end{aligned} \quad (1)$$

where  $u_1(t) = a(t) + jb(t)$  and  $u_2(t) = c(t) + jd(t)$  are the considered complex baseband information signals, both with the same bandwidth  $B$ , and carrier frequencies  $\omega_{c1}$  and  $\omega_{c2}$ , respectively. If we focus on the first signal,  $i_1(t)$ , and determine its Fourier transform (FT), we arrive at

$$\begin{aligned} I_1(\omega) &= \frac{1}{2}[A(\omega) + jB(\omega)] * \delta(\omega - \omega_{c1}) \\ &+ \frac{1}{2}[A(\omega) - jB(\omega)] * \delta(\omega + \omega_{c1}), \end{aligned} \quad (2)$$

being  $*$  the convolution operator,  $\delta(\omega)$  the unit impulse in the frequency domain,  $A(\omega)$  and  $B(\omega)$  the FT of the real-valued signals  $a(t)$  and  $b(t)$ , which satisfy  $A(\omega) = A^*(-\omega)$  and  $B(\omega) = B^*(-\omega)$ , with  $*$  denoting the complex conjugate operator. From Eq. (2) we define  $A(\omega) + jB(\omega) = U_1(\omega)$ , with  $U_1(\omega) = \text{FT}[u_1(t)]$ , and  $A(\omega) - jB(\omega) = A^*(-\omega) - jB^*(-\omega) = U_1^*(-\omega)$ , and Eq. (2) is rewritten as

$$I_1(\omega) = \frac{1}{2}[U_1(\omega - \omega_{c1}) + U_1^*(-(\omega + \omega_{c1}))]. \quad (3)$$

Following the same simple steps for the determination of the FT of the rest of the signals in Eq. (1) we obtain:

$$\begin{aligned} Q_1(\omega) &= \frac{1}{2}[jU_1(\omega - \omega_{c1}) - jU_1^*(-(\omega + \omega_{c1}))], \\ I_2(\omega) &= \frac{1}{2}[U_2(\omega - \omega_{c2}) + U_2^*(-(\omega + \omega_{c2}))], \text{ and} \\ Q_2(\omega) &= \frac{1}{2}[-jU_2(\omega - \omega_{c2}) + jU_2^*(-(\omega + \omega_{c2}))]. \end{aligned} \quad (4)$$

Considering Eq. (3) and Eq. (4), the magnitude spectra of  $i(t) = i_1(t) + i_2(t)$  and  $q(t) = q_1(t) + q_2(t)$  (see Fig. 2) are represented in Fig. 4(a) and (b), respectively.

Let us consider the analytic representation of  $i(t)$  and  $q(t)$  (see Fig. 4 and Eqs. (3) and (4)) given by

$$\begin{aligned} \tilde{i}(t) &= \frac{1}{2}[u_1(t)e^{j\omega_{c1}t} + u_2(t)e^{j\omega_{c2}t}] \text{ and} \\ \tilde{q}(t) &= \frac{1}{2}[ju_1(t)e^{j\omega_{c1}t} - ju_2(t)e^{j\omega_{c2}t}], \end{aligned} \quad (5)$$

where we notice that, as a result of the complex mixing, we obtain two types of signals: 1)  $\tilde{i}(t)$  consisting of the original signals located at the corresponding carrier frequencies, and 2)

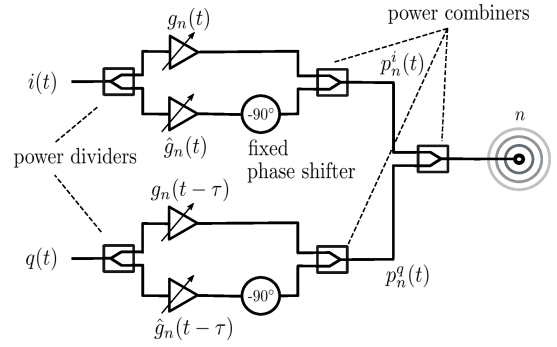


Fig. 3. Block diagram of the dual-input  $n$ -th antenna element of the proposed dual-input SSB transmit TMA. The output signals  $i(t)$  and  $q(t)$  of the dual complex mixer shown in Fig. 2 are distributed to all SSB TMA dual-input antenna elements. Notice that the time-modulation implementation employs VGAs with digital control but there are other possibilities as well [2].

$\tilde{q}(t)$  containing phase-shifted versions of  $u_1(t)$  (shifted  $\pi/2$ ) and  $u_2(t)$  (shifted  $-\pi/2$ ). Notice that this feature avoids RF crosstalk or coupling between both channels (especially in miniaturized circuits) at the antenna ports.

## III. DUAL-INPUT SSB TRANSMIT TMA

The proposed system consists of a dual complex mixer connected to a dual-input SSB TMA, as shown in Fig. 2. Fig. 3 shows the block diagram of each TMA antenna element, where  $g_n(t)$  and  $\hat{g}_n(t)$  are periodic ( $T_0$ ) pulses ( $\hat{g}_n(t)$  is the HT of  $g_n(t)$ ) and  $\tau$  is a time delay.

This TMA architecture would allow for accomplishing high levels of beamforming flexibility (compared to switched TMAs and interleaved arrays) and efficiency (compared to switched TMAs), offering also a competitive cost (with respect to schemes based on multibeam phased arrays at the expense of a higher power consumption) and software simplicity (compared to switched TMAs and interleaved arrays at the cost of a hardware complexity increase).

The modulating pulses are synthesized from a periodic rectangular sequence  $r_n(t)$  (see Fig. 5) as follows: 1) the direct current (DC) component of  $r_n(t)$  (which corresponds to its Fourier series coefficient  $G_{n0} = \tau_n/T_0 = \xi_n$  [3], where  $\tau_n$  is its time-width) is filtered; 2) a dual complex modulation is applied to such a DC signal in order to shift both the time-linear control of the amplitudes (given by  $\xi_n$ ) and the time control of the phases (given by the time delays  $\delta_{nm}$ ) to the

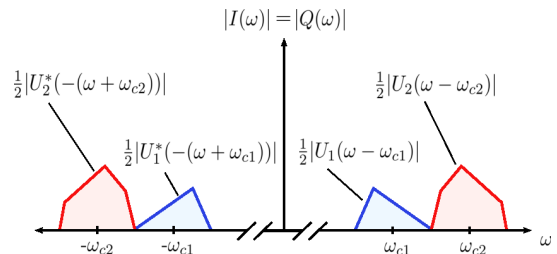


Fig. 4. Magnitude spectra of  $i(t) = i_1(t) + i_2(t)$  and  $q(t) = q_1(t) + q_2(t)$  at the output of the dual complex mixer in Fig. 2. The carrier frequencies obey  $\omega_{c2} = \omega_{c1} + B$ , where  $B$  is the baseband signal bandwidth.

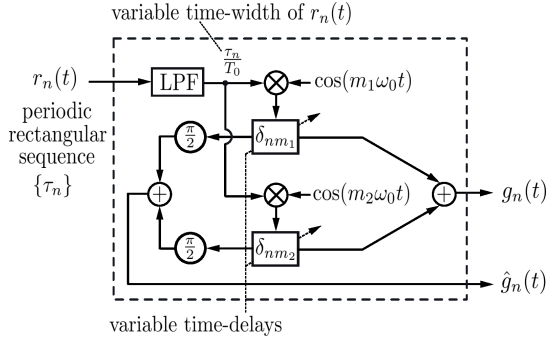


Fig. 5. Block diagram of the pre-processing of a periodic rectangular pulse [8] to synthesize the two quadrature periodic pulses that govern the  $n$ -th antenna element of the transmit TMA shown in Fig. 3. LPF stands for low-pass filter.

spectral lines at frequencies  $m\omega_0$ , with  $m \in \mathcal{P} = \{m_1, m_2\}$  and  $\omega_0 = 2\pi/T_0$ . We assume that

$$\begin{aligned} m_1 &\text{ is an odd natural number, and} \\ m_2 &= (m_1 + 2) + 4k, \text{ with } k \in \mathbb{N}. \end{aligned} \quad (6)$$

The expressions for the obtained pulses are trivially derived from Fig. 5 and are given, respectively, by

$$\begin{aligned} g_n(t) &= \sum_{m \in \mathcal{P}} \xi_n \cos(m\omega_0(t - \delta_{nm})), \text{ and} \\ \hat{g}_n(t) &= \sum_{m \in \mathcal{P}} \xi_n \sin(m\omega_0(t - \delta_{nm})). \end{aligned} \quad (7)$$

We will prove in the ensuing section that if these pulses and their time-shifted versions  $g_n(t - \tau)$  and  $\hat{g}_n(t - \tau)$  operate in compliance with the scheme in Fig. 3 to transmit the signals in Eq. (5) (constructed according to Fig. 2), it is then possible to confine the radiated energy in a pair of positive harmonic patterns located at carrier frequencies  $\omega_c + m\omega_0$ . As a consequence, it is possible to transmit each original information signal,  $u_1(t)$  and  $u_2(t)$ , over each independently reconfigurable pattern.

#### IV. SIGNALS RADIATED BY THE TMA

The analytic representation of the compound signal radiated by the TMA in Fig. 3 is given by

$$\tilde{s}_{\text{rad}}(t, \theta) = \sum_{n=0}^{N-1} [\tilde{p}_n^i(t) + \tilde{p}_n^q(t)] e^{jkz_n \cos \theta}, \quad (8)$$

where  $[\tilde{p}_n^i(t) + \tilde{p}_n^q(t)] e^{jkz_n \cos \theta}$  is the signal radiated by the  $n$ -th element of the TMA. By virtue of the scheme in Fig. 3, the pair of time-modulated signals in the array is

$$\begin{aligned} \tilde{p}_n^i(t) &= \tilde{i}(t)[g_n(t) - j\hat{g}_n(t)], \text{ and} \\ \tilde{p}_n^q(t) &= \tilde{q}(t)[g_n(t - \tau) - j\hat{g}_n(t - \tau)], \end{aligned} \quad (9)$$

being

$$\begin{aligned} \tilde{P}_n^i(\omega) &= \frac{1}{2\pi} \tilde{I}(\omega) * [G_n(\omega) - j\hat{G}_n(\omega)], \text{ and} \\ \tilde{P}_n^q(\omega) &= \frac{1}{2\pi} \tilde{Q}(\omega) * [e^{-j\omega\tau}(G_n(\omega) - j\hat{G}_n(\omega))] \end{aligned} \quad (10)$$

their respective FTs. Considering Eq. (5),  $\tilde{I}(\omega) = \text{FT}[\tilde{i}(t)] = \frac{1}{2}[U_1(\omega - \omega_{c1}) + U_2(\omega - \omega_{c2})]$  and  $\tilde{Q}(\omega) = \text{FT}[\tilde{q}(t)] =$

$\frac{1}{2}[jU_1(\omega - \omega_{c1}) - jU_2(\omega - \omega_{c2})]$ . It follows from Eq. (7) that

$$\begin{aligned} G_n(\omega) &= \text{FT}[g_n(t)] \\ &= \pi \xi_n \sum_{m \in \mathcal{P}} [e^{-jm\omega_0\delta_{nm}} \delta(\omega - m\omega_0) + e^{jm\omega_0\delta_{nm}} \delta(\omega + m\omega_0)], \\ \hat{G}_n(\omega) &= \text{FT}[\hat{g}_n(t)] \\ &= \frac{\pi \xi_n}{j} \sum_{m \in \mathcal{P}} [e^{-jm\omega_0\delta_{nm}} \delta(\omega - m\omega_0) - e^{jm\omega_0\delta_{nm}} \delta(\omega + m\omega_0)]. \end{aligned} \quad (11)$$

By considering the previous expressions, and denoting  $\Phi_{nm} = m\omega_0\delta_{nm}$ , the following equality holds

$$G_n(\omega) - j\hat{G}_n(\omega) = 2\pi \xi_n \sum_{m \in \mathcal{P}} e^{j\Phi_{nm}} \delta(\omega + m\omega_0). \quad (12)$$

Consequently, if we select a delay  $\tau$  verifying that  $\omega_0\tau = \pi/2$ , then  $e^{-jm\omega_0\tau} = (-j)^m$ , and Eq. (10) can be rewritten as

$$\begin{aligned} \tilde{P}_n^i(\omega) &= \frac{\xi_n}{2} \sum_{m \in \mathcal{P}} e^{j\Phi_{nm}} [U_1(\omega - (\omega_{c1} - m\omega_0)) \\ &\quad + U_2(\omega - (\omega_{c2} - m\omega_0))], \text{ and} \\ \tilde{P}_n^q(\omega) &= \frac{\xi_n}{2} \sum_{m \in \mathcal{P}} e^{j\Phi_{nm}} (-j)^m [jU_1(\omega - (\omega_{c1} - m\omega_0)) \\ &\quad - jU_2(\omega - (\omega_{c2} - m\omega_0))], \end{aligned} \quad (13)$$

which leads to

$$\begin{aligned} \tilde{P}_n^i(\omega) + \tilde{P}_n^q(\omega) &= \frac{\xi_n}{2} \sum_{m \in \mathcal{P}} e^{j\Phi_{nm}} [(1 - j^{m+1})U_1(\omega - (\omega_{c1} - m\omega_0)) \\ &\quad + (1 + j^{m+1})U_2(\omega - (\omega_{c2} - m\omega_0))]. \end{aligned} \quad (14)$$

By considering Eq. (6),  $j^{m_1+1} = -1$  and  $j^{m_2+1} = 1$ , and selecting  $\omega_{c1} = \omega_c + m_1\omega_0$  and  $\omega_{c2} = \omega_c + m_2\omega_0$  (see Fig. 2), the sum in Eq. (14) becomes

$$\begin{aligned} \tilde{P}_n^i(\omega) + \tilde{P}_n^q(\omega) &= \xi_n e^{j\Phi_{nm_1}} U_1(\omega - \omega_c) \\ &\quad + \xi_n e^{j\Phi_{nm_2}} U_2(\omega - \omega_c). \end{aligned} \quad (15)$$

Notice that the signals at  $\omega_c$  are added constructively, whereas the signals at  $\omega_c \pm (m_2 - m_1)\omega_0$  are added destructively, due to the combination of complex mixing followed by time modulation. In order to avoid signal spectral overlapping (see Fig. 4), the condition  $\omega_{c2} - \omega_{c1} = (m_2 - m_1)\omega_0 > B$  must be fulfilled. Considering Eq. (8) and the inverse FT of Eq. (15), the signal radiated over the TMA in the time domain is

$$\begin{aligned} \tilde{s}_{\text{rad}}(t, \theta) &= \sum_{n=0}^{N-1} \xi_n e^{j\Phi_{nm_1}} e^{jkz_n \cos \theta} u_1(t) e^{j\omega_c t} \\ &\quad + \sum_{n=0}^{N-1} \xi_n e^{j\Phi_{nm_2}} e^{jkz_n \cos \theta} u_2(t) e^{j\omega_c t}, \end{aligned} \quad (16)$$

and since the spatial array factor corresponding to the harmonic or order  $m$  is given by  $F_m^{\text{TMA}}(\theta) = \sum_{n=0}^{N-1} \xi_n e^{j\Phi_{nm}} e^{jkz_n \cos \theta}$  [8], we finally have

$$\tilde{s}_{\text{rad}}(t, \theta) = u_1(t) e^{j\omega_c t} F_{m_1}^{\text{TMA}}(\theta) + u_2(t) e^{j\omega_c t} F_{m_2}^{\text{TMA}}(\theta), \quad (17)$$

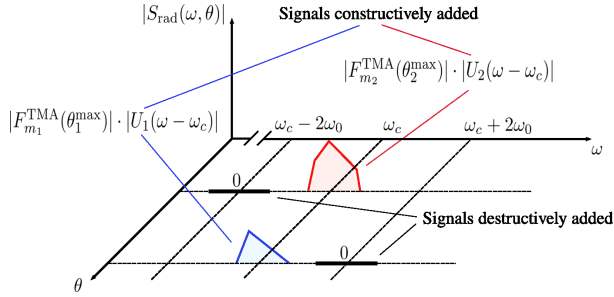


Fig. 6. Magnitude spectra of the radiated signals contemplating both the spatial and the frequency domains (FT of Eq. (17)). Notice that the TMA pulses are designed to exploit their first ( $m_1 = 1$ ) and third ( $m_2 = 3$ ) order harmonics. It is shown (according to Eq. (14)) how the TMA processing, together with the complex mixing, allows for canceling out the information signals located at  $\omega_c \pm 2\omega_0$ , thus guaranteeing transmit power efficiency.

where it is shown that, thanks to this technique, each information signal,  $u_1(t)$  and  $u_2(t)$ , is simultaneously transmitted over the same frequency and the same physical antenna array with the extra feature of providing such signals with independent time-controlled spatial signatures  $F_{m_1}^{\text{TMA}}(\theta)$  and  $F_{m_2}^{\text{TMA}}(\theta)$ .

## V. EXAMPLE

In this section we illustrate the operating principle of the proposed technique. We start considering the periodical pulses Eq. (7) and selecting the harmonics  $m_1 = 1$  and  $m_2 = 3$ . Fig. 6 shows the magnitude spectra of the signals radiated simultaneously over the spatial and frequency domains. We have considered, as a graphical example, the pre-processed signals illustrated in Fig. 4. The radiated signal follows the FT of Eq. (17). According to Eq. (14), the TMA processing, together with the complex mixing, locate  $U_1(\omega)$  at  $\omega_{c1} - m_1\omega_0$  and  $\omega_{c1} - m_2\omega_0$ , and the signal  $U_2$  at  $\omega_{c2} - m_1\omega_0$  and  $\omega_{c2} - m_2\omega_0$ , and this allows for canceling out the information signals located at  $\omega_c \pm 2\omega_0$ , while adding constructively the signals at  $\omega_c$ , thus guaranteeing an efficient power transmission.

On the other hand, let us see the versatility offered by the proposed technique in terms of the spatial signature provided to the signals. We consider a TMA with  $N = 20$  elements (each one in accordance with the structure in Fig. 3) linearly spaced  $d = \lambda/2$ . In Fig. 7 we show the TMA radiated pattern for two scenarios. In the first one (at the time instant  $t = t_0$ ) the maxima of the first and the third harmonic patterns point to each of the receivers, located at  $\theta_1 = 40^\circ$  and  $\theta_3 = 130^\circ$ , respectively, with an identical gain  $G = 15.8$  dB. The  $\xi_n$  are selected to transform the static uniform pattern into a normalized Gaussian pattern with a standard deviation of  $4/5$  (with a  $-19$  dB side-lobe level (SLL) pattern). At the time instant  $t = t_1$ , we consider a second scenario where the receivers have moved to the directions  $\theta_1 = 75^\circ$  and  $\theta_3 = 92^\circ$  ( $G = 15.4$  dB). In this case, the  $\xi_n$  are reconfigured to synthesize a 30 dB Dolph-Chebyshev pencil beam pattern. The theoretical power efficiency of the TMA (note that the hardware efficiency [2] is not considered because it depends on the specific devices) in both cases is calculated as in [8] and is  $\eta(L) = 100\%$ .

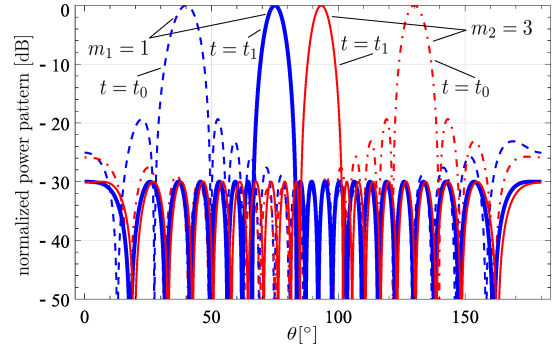


Fig. 7. Radiation power patterns of an SSB transmit TMA with the structure proposed in Fig. 3. The versatility of the pre-processed rectangular pulses in Eq. (7), exploiting their first ( $m_1 = 1$ ) and third ( $m_2 = 3$ ) order harmonics, allows for moving from an SLL-relaxed scenario (dashed lines) at  $t = t_0$  ( $\theta_1 = 40^\circ$ ,  $\theta_3 = 130^\circ$ ) to another at  $t = t_1$  (solid lines) where the presence of pencil beam patterns is necessary ( $\theta_1 = 75^\circ$ ,  $\theta_3 = 92^\circ$ ).

## VI. CONCLUSIONS

We have proposed an innovative transmit beamforming scheme based on two complementary operations: complex mixing of baseband signals and TMA processing with quadrature and time-delayed periodic pulses. We focused on an elementary design capable of simultaneously transmitting – over the same TMA – two different information signals using independent time-controlled harmonic patterns. There is room for future research on exploiting the functionalities of TMAs at transmission (e.g., diversity and multi-user purposes) especially when acting in conjunction with signal precoding. The generalization to an analog precoding scheme handling more than two signals is left as a future work.

## REFERENCES

- [1] P. Rocca, G. Oliveri, R. J. Mailloux, and A. Massa, “Unconventional phased array architectures and design methodologies: A review,” *Proc. IEEE*, vol. 104, no. 3, pp. 544–560, Mar. 2016.
- [2] R. Maneiro-Catoira, J. Brégains, J. A. García-Naya, and L. Castedo, “Enhanced time-modulated arrays for harmonic beamforming,” *IEEE J. Sel. Topics Signal Process.*, vol. 11, no. 2, pp. 259–270, Mar. 2017.
- [3] J. Brégains, J. Fondevila-Gomez, G. Franceschetti, and F. Ares, “Signal radiation and power losses of time-modulated arrays,” *IEEE Trans. Antennas Propag.*, vol. 56, no. 6, pp. 1799–1804, 2008.
- [4] Q. Zhu, S. Yang, R. Yao, M. Huang, and Z. Nie, “Unified time- and frequency-domain study on time-modulated arrays,” *IEEE Trans. Antennas Propag.*, vol. 61, no. 6, pp. 3069–3076, June 2013.
- [5] R. Maneiro-Catoira, J. Brégains, J. García-Naya, and L. Castedo, “On the feasibility of time-modulated arrays for digital linear modulations: A theoretical analysis,” *IEEE Trans. Antennas Propag.*, vol. 62, no. 12, pp. 6114–6122, Dec. 2014.
- [6] P. Rocca, Q. Zhu, E. Bekele, S. Yang, and A. Massa, “4-D arrays as enabling technology for cognitive radio systems,” *IEEE Trans. Antennas Propag.*, vol. 62, no. 3, pp. 1102–1116, Mar. 2014.
- [7] C. He, X. Liang, B. Zhou, J. Geng, and R. Jin, “Space-division multiple access based on time-modulated array,” *IEEE Antennas Wireless Propag. Lett.*, vol. 14, pp. 610–613, 2015.
- [8] R. Maneiro-Catoira, J. Brégains, J. A. García-Naya, and L. Castedo, “Analog beamforming using time-modulated arrays with digitally preprocessed rectangular sequences,” *IEEE Antennas Wireless Propag. Lett.*, vol. 17, no. 3, pp. 497–500, Mar. 2018.